

# Surface-Plasmon Resonance for Photoluminescence and Solar-Cell Applications

Jongmin Kim,<sup>†</sup> Hongsik Choi,<sup>†</sup> Changwoo Nahm,<sup>†</sup> and Byungwoo Park<sup>\*</sup>

WCU Hybrid Materials Program, Department of Materials Science and Engineering, Research Institute of Advanced Materials, Seoul National University, Seoul 151-744, Korea

The surface plasmon of metal nanostructures influences surrounding semiconductors in various ways. In particular, a surface plasmon modifies recombination rates of excitons in a semiconductor, and intensifies photon flux in the vicinity of metal nanostructures. These phenomena have contributed to the improvement of photoluminescent properties both by enhancement of radiative recombination and by electromagnetic-field amplification, even though the degree of nonradiative energy dissipation is sensitively dependent on the metal-semiconductor distance. Strong light absorption induced by surface plasmons is also attractive for photovoltaic applications, so metal nanostructures can be incorporated into diverse solar-cell systems with a reduced solar-cell thickness.

**Keywords:** surface plasmon, photoluminescence, solar cell, nanoparticle

## 1. SURFACE-PLASMON RESONANCE

### 1.1 Introduction

Surface plasmons are the collective oscillation of electrons that propagate through a metal/dielectric interface. At the metal/dielectric interface, the electrons are excited by the electromagnetic field, and the interactions between surface electrons and electromagnetic field constitute the surface plasmon. The schematic illustration of a surface plasmon is

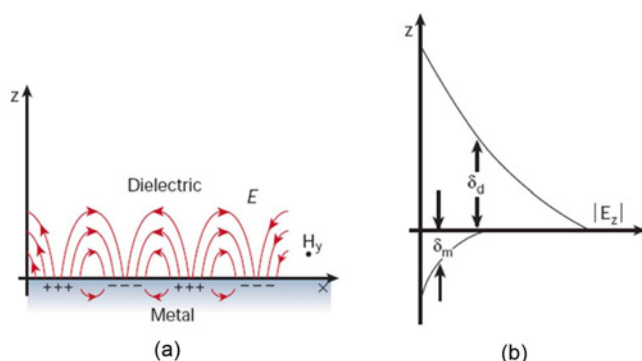


**Fig. 1.** (a) The charges and electromagnetic field of the surface plasmon propagating through a surface in the  $x$  direction are shown schematically. (b) The exponential dependence of the electric field ( $E_z$ ). Reprinted with permission from W. L. Barnes, A. Dereux, and T. W. Ebbesen.<sup>[1]</sup> Copyright 2003, Nature Publishing Group.

shown in Fig. 1(a). The electric field from oscillating electrons at the metal surface decays exponentially in the dielectric medium (Fig. 1(b)). The dispersion relations of surface plasmons can be obtained by solving Maxwell's equations. In the case of a 2-D metal/dielectric interface, the dispersion relation becomes:<sup>[1]</sup>

$$k = \frac{\omega}{c} \sqrt{\frac{\epsilon_d \epsilon_m}{\epsilon_d + \epsilon_m}} \quad (1-1)$$

where  $k$ ,  $\omega$ , and  $c$  are wavevector, angular frequency, and light velocity, respectively, and  $\epsilon_d$  and  $\epsilon_m$  are the frequency-dependent permittivity of dielectric materials and metal, respectively. As shown in Fig. 2 demonstrating the dispersion relations  $\omega(k)$  vs.  $k$ , the momentum ( $\hbar k$ ) of a surface plasmon is larger than that of the light-dispersion relation.<sup>[2]</sup> For this reason, the coupling of light and surface plasmon does not always happen. However, surface plasmons propagating along a grating or a rough surface can satisfy the momentum conservation with the incident photon, so that the surface plasmons become excited by light waves.<sup>[2]</sup>

Metal nanostructures strongly interact with photons which have similar energy with their plasmon-resonance energy. For example, an aluminum nanoparticle of 13 nm diameter has a surface-plasmon resonance energy of  $\sim 8.8$  eV, and its absorption efficiency for light of energy 8.8 eV is 18,<sup>[3]</sup> which means that its cross section for absorption is 18 times greater than its geometrical cross section. Field lines of the Poynting vector illustrate the photon paths, as shown in Fig. 3. The strong convergence of field lines near the nano-

\*Corresponding author: byungwoo@snu.ac.kr

<sup>†</sup>Three authors contributed equally to this work.

©KIM and Springer

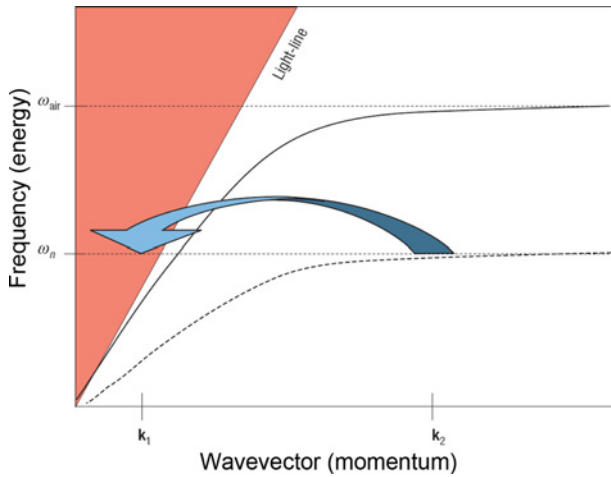


**Fig. 2.** Dispersion relation of the surface plasmon and the light line. Reprinted with permission from W. L. Barnes.<sup>[2]</sup> Copyright 2004, Nature Publishing Group.

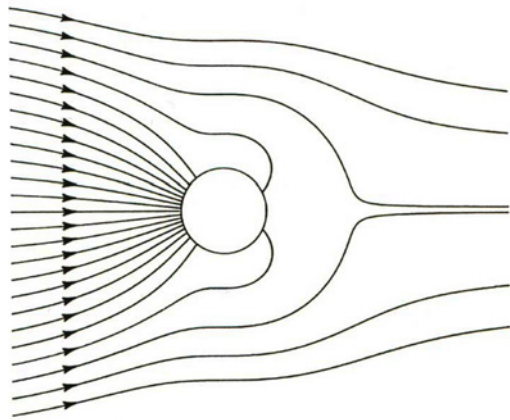


**Fig. 3.** Field lines of the total Poynting vector around an aluminum nanoparticle illuminated by 8.8 eV photon, which is the surface-plasmon resonance energy of an aluminum nanoparticle. From Ref. [3].

particle indicates that light passing near the metal deflects toward it, that is, light is strongly absorbed by the nanoparticle.

**1.2 Surface-Plasmon Effect on the Luminescence Properties**

In recent years, compound semiconductor nanoparticles have been widely researched as luminescent materials,<sup>[4-24]</sup> and various attempts have been conducted to enhance their luminescent properties by modification of the density of states in the excitation and emission modes.<sup>[25-36]</sup> The optical properties of semiconductors are affected by nearby metal nanostructures. Mostly, the surface plasmon enhances the luminescence properties in two ways: modification of radiative/nonradiative recombination rates, and localized-field enhancement. First, the radiative/nonradiative recombination rates of a semiconductor can be controlled by the nearby metal nanostructures. The schematic diagram of how the surface-plasmon coupling occurs is shown in Fig. 4.<sup>[37]</sup>

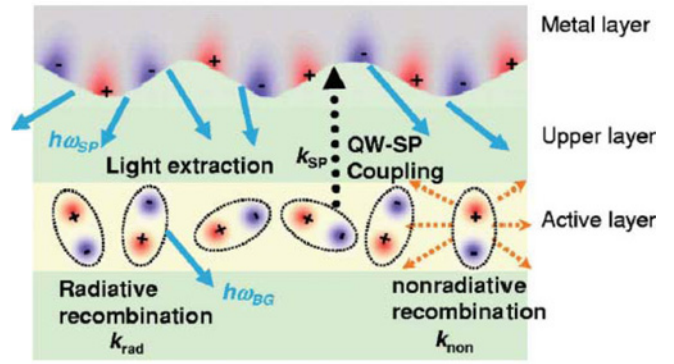


**Fig. 4.** Schematic diagram of the electron-hole recombination and quantum-well (QW) surface-plasmon coupling mechanisms. Reprinted with permission from K. Okamoto.<sup>[37]</sup> Copyright 2011, American Institute of Physics.

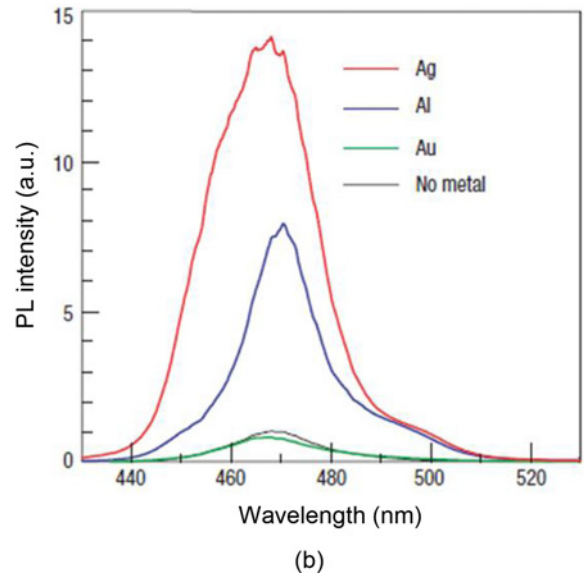
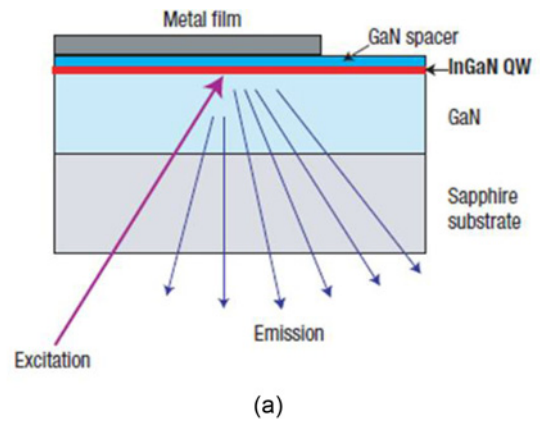


**Fig. 5.** (a) Sample structure and excitation/emission configuration of photoluminescence, and (b) photoluminescence spectra of InGaN/GaN quantum well (QW) coated with Ag, Al, Au, and no metal. The distance between the metal layer and QW was 10 nm. Reprinted with permission from A. Scherer.<sup>[38]</sup> Copyright 2004, Nature Publishing Group.

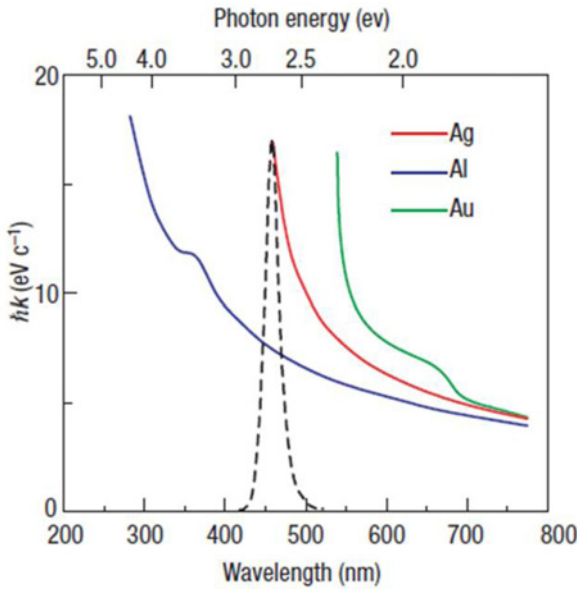


**Fig. 6.** Dispersion diagrams of surface plasmons generated on Ag/GaN, Al/GaN, and Au/GaN surfaces. Wavevector of the surface plasmon is denoted as  $k$ , and the dashed line is the photoluminescence spectrum of InGaN/GaN. Reprinted with permission from A. Scherer.<sup>[38]</sup> Copyright 2004, Nature Publishing Group.

When the semiconductor absorbs the incident light, excitons in the semiconductor interact with the surface plasmons of metal nanostructures.

Scherer’s group examined the photoluminescence of an InGaN quantum well (QW) that was coated with various metal layers and ~10 nm GaN spacer.<sup>[38]</sup> With an appropriate selection of metal, the photoluminescence from the quantum well layer increased by one order of magnitude (Fig. 5). They correlated the increased luminescence with the dispersion relation for the surface plasmon of various metals (Fig. 6): the surface-plasmon energy of an Ag layer matches well with the InGaN emitter, thereby a large increase of luminescence intensity is observed. In the case of an Au layer, however, there is no surface-plasmon mode at the emission energy of the nearby semiconductor, so the photoluminescence intensity is not affected.

As for the localized-field enhancement, the enhanced field is induced by the localization of the electromagnetic field in the vicinity of metal nanostructures. The enhancement factor  $\eta$  (intensity ratio of the resultant to incident field) can be calculated assuming one isotropic metal sphere is placed in a homogeneous medium:<sup>[39]</sup>

$$\eta = \frac{|\vec{E}_2|^2}{|\vec{E}_0|^2} = \left( \left| 1 + 2 \frac{a^3}{r^3} \frac{\epsilon_{metal} - \epsilon_{medium}}{\epsilon_{metal} + 2\epsilon_{medium}} \right|^2 \cos^2 \theta + \left| -1 + \frac{a^3}{r^3} \frac{\epsilon_{metal} - \epsilon_{medium}}{\epsilon_{metal} + 2\epsilon_{medium}} \right|^2 \sin^2 \theta \right) \quad (1-2)$$

where  $\epsilon_{metal}$  and  $\epsilon_{medium}$  are the dielectric constants of the metal

nanoparticle and the surrounding medium, respectively, and  $a$  and  $r$  are the radius of the metal nanoparticle and the distance from the center of the metal nanoparticle, respectively. Figure 7 shows the field enhancement factor of an Au nanoparticle at the wavelength of 550 nm. Excitation of the localized surface plasmons in metal nanoparticles accelerates the creation of electron-hole pairs in the semiconductor.<sup>[40]</sup> As shown in Fig. 8, dye-adsorbed TiO<sub>2</sub> photoelectrode absorbs more light when silver nanoparticles are contained in the electrode, due to the localized-field enhancement.<sup>[41]</sup>

On the other hand, a surface plasmon near a semiconductor also affects the nonradiative recombination rate by energy dissipation. Once the distance of metal and semiconductor

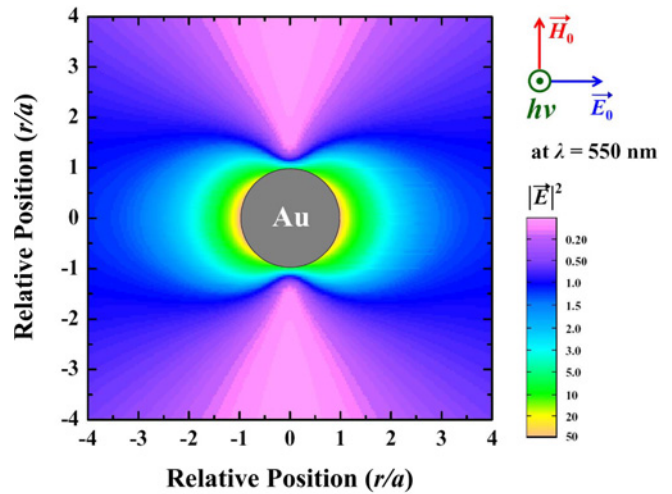


**Fig. 7.** Calculated field-enhancement factor of Au nanoparticle. The dielectric constants of metal and surrounding medium are  $-5.181 + 2.094 \cdot i$  and  $2.220 + 0 \cdot i$ , respectively. From Ref. [40].

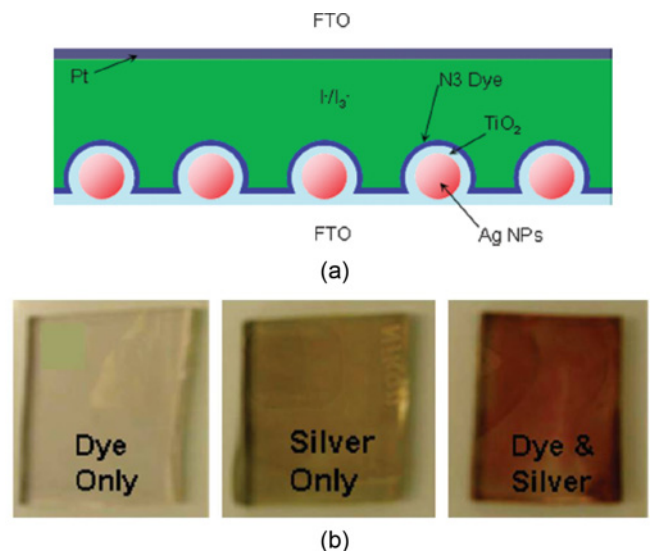


**Fig. 8.** (a) Configuration of solar cells containing silver nanoparticles and dye, and (b) photos of anodes showing the enhancement of light absorption by the introduction of Ag. From Ref. [41].

gets close enough, energy transfer between the semiconductor and metal occurs, so that the electron-hole pair recombines nonradiatively. Schematic illustrations of energy transfer from semiconductor to metal are shown in Fig. 9(a),<sup>[42]</sup> and this energy-transfer time lies approximately within the 0.1 - 1 ns range (Fig. 9(b)).<sup>[43-46]</sup> Therefore, the degree of nonradiative energy dissipation is strongly dependent on the

metal-semiconductor distance. Due to this nonradiative effect, fluorescence intensity shows an optimum efficiency at an appropriate metal-semiconductor distance.<sup>[47-49]</sup> The effect from an isolated Au nanoparticle on the fluorescence rate of a single molecule emitter was calculated considering both the localized-field enhancement and the nonradiative energy-transfer loss (Fig. 10). The fluorescence

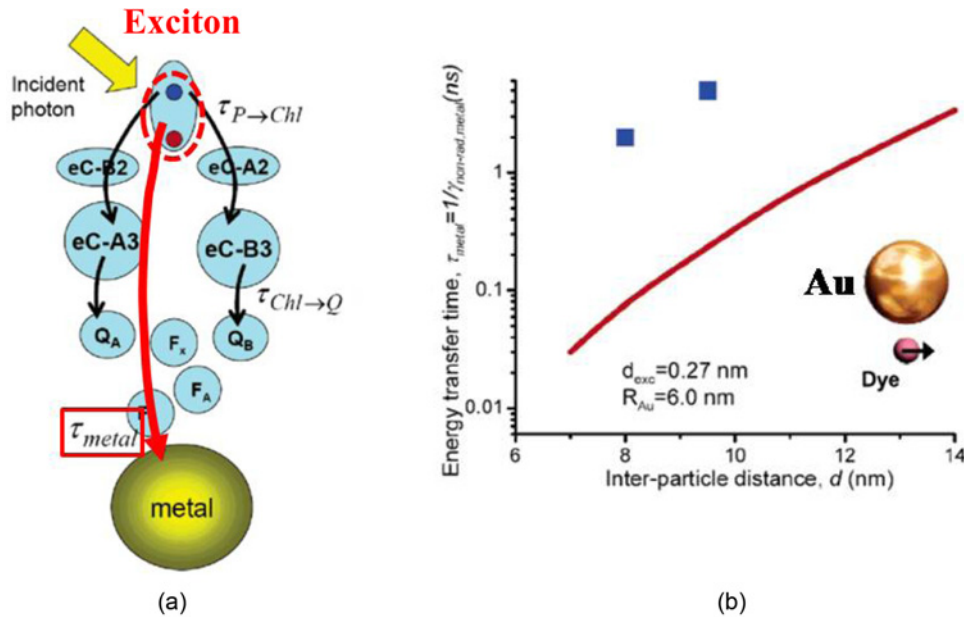


**Fig. 9.** (a) A schematic diagram of energy transfer (quenching) to metal. From Ref. [42]. (b) Energy-transfer time as a function of the distance between dye molecule and Au nanoparticle. The curves are obtained by numerical analysis, and the square symbols represent experimental data. From Ref. [43].

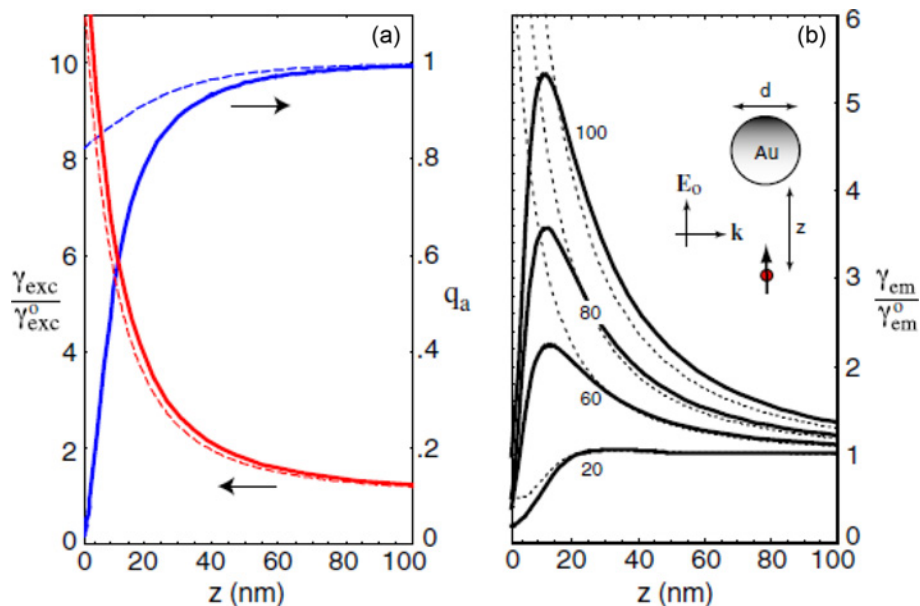


**Fig. 10.** Calculated quantum yield  $q_a$ , excitation rate  $\gamma_{exc}$ , and fluorescence rate  $\gamma_{em}$  as a function of molecule-particle separation. The  $\gamma_{exc}$  and  $\gamma_{em}$  are normalized by their corresponding free-space values ( $z \rightarrow \infty$ ). The solid curves are the results of calculations whereas the dashed ones correspond to the dipole approximation which fails for short distance  $z$ . In (a) the particle diameter is  $d = 80$  nm, and in (b) Au diameters are indicated in the figure. Excitation wavelength is  $\lambda = 650$  nm, and  $\epsilon = -12.99 + 1.09 \cdot i$  (gold).<sup>[50]</sup> Copyright 2006 by the American Physical Society.

exhibits a maximum at a distance between metal and molecular emitter of ~10 nm, and these calculations correlate well with experimental results.<sup>[50]</sup> However, they did not consider the influence of the radiative recombination rate as a function of metal-semiconductor distance.

## 2. PHOTOLUMINESCENCE ENHANCEMENT IN SEMICONDUCTOR NANOPARTICLES BY SURFACE-PLASMON RESONANCE

### 2.1 Introduction

The important factors determining surface-plasmon resonance are the metal-semiconductor distance and energy matching between the surface plasmon and semiconductor emitter. The metal-semiconductor distance has an influence on the radiative and nonradiative energy-transfer rates. Energy matching is also important because the emission of semiconductor must be located close to the surface-plasmon energy for an effective surface-plasmon resonance. The density of surface-plasmon states can be also tuned for efficient energy matching.

### 2.2 Surface-Plasmon Resonance in Colloidal Mixtures of Semiconductor/Metal Nanoparticles

To investigate radiative/nonradiative recombination rates and quantum efficiency as a function of metal-semiconductor distance, the CdS and Au nanoparticles were investigated in colloidal mixtures with various molar fractions.<sup>[51]</sup> As shown in Fig. 11, photoluminescence intensities improved with increasing gold fraction, and a mole fraction of 10:1 resulted in the strongest emission peak. As expected, the luminescence intensity started to decrease at higher Au frac-

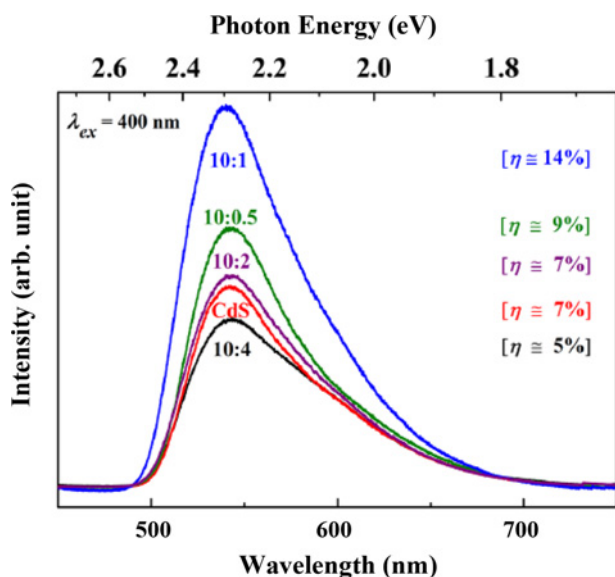


**Fig. 11.** Photoluminescence spectra of mixed CdS/Au nanoparticles with various CdS/Au mole fractions. Reprinted with permission from B. Park.<sup>[51]</sup> Copyright 2011, American Institute of Physics.

tions, indicating the existence of an optimum resonance distance between metal and semiconductor.<sup>[52]</sup>

The radiative and nonradiative recombination rates can be easily determined considering the total recombination rate and quantum efficiency when the time-resolved photoluminescence shows single-exponential decay behavior. The quantum efficiency ( $\eta$ ) is the ratio of the radiative recombination to the total recombination:

$$\eta = \frac{k_{rad}}{k_{rad} + k_{nonrad}} = k_{rad} \times \tau \tag{2-1}$$

where  $k_{rad}$ ,  $k_{nonrad}$ , and  $\tau$  are the radiative, nonradiative recombination rates, and decay time respectively. Obvious correlations between the quantum efficiency and radiative/nonradiative recombination rate are shown in Fig. 12. The incorporated gold nanoparticles promote the radiative recombination indicating that surface-plasmon resonance accelerates the radiative recombination of electron-hole pair. However, when a metal is in close proximity to a semiconductor or other metal, destructive interference occurs, and consequently, a decrease in the luminescence efficiency is observed at higher Au fractions.<sup>[37]</sup>

Figure 13 shows the schematics of a possible mechanism of resonance between surface plasmon and exciton. If there are no Au nanoparticles around the CdS nanoparticles, nonradiative recombination is dominant with the quantum efficiency of ~10%. Radiative recombination of an electron-hole pair is dominant when Au nanoparticles are present at an appropriate distance (several tens of nanometers) from the CdS nanoparticles,<sup>[53]</sup> and the emission energy of the CdS nanoparticles matches well with the surface plasmon of Au nanoparticles. On the other hand, if the amount of Au becomes too high, the nonradiative energy transfer between CdS and Au occurs, and also destructive interferences of surface plasmons become dominant due to the metal-metal nanoparticle distance.

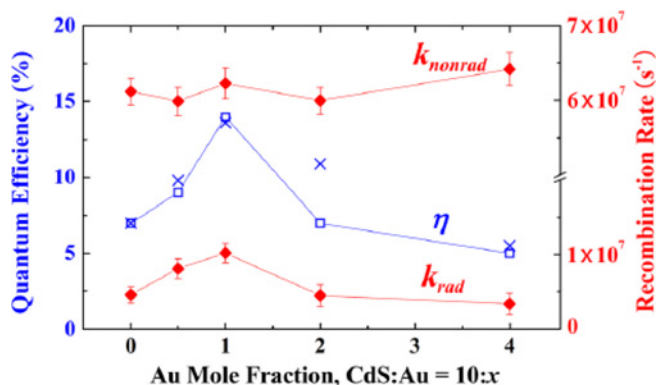


**Fig. 12.** Quantum efficiency, radiative recombination rate, and nonradiative recombination rate of the CdS/Au mixtures with various mole fractions. The estimated quantum efficiency is also shown (× symbol). Reprinted with permission from B. Park.<sup>[51]</sup> Copyright 2011, American Institute of Physics.

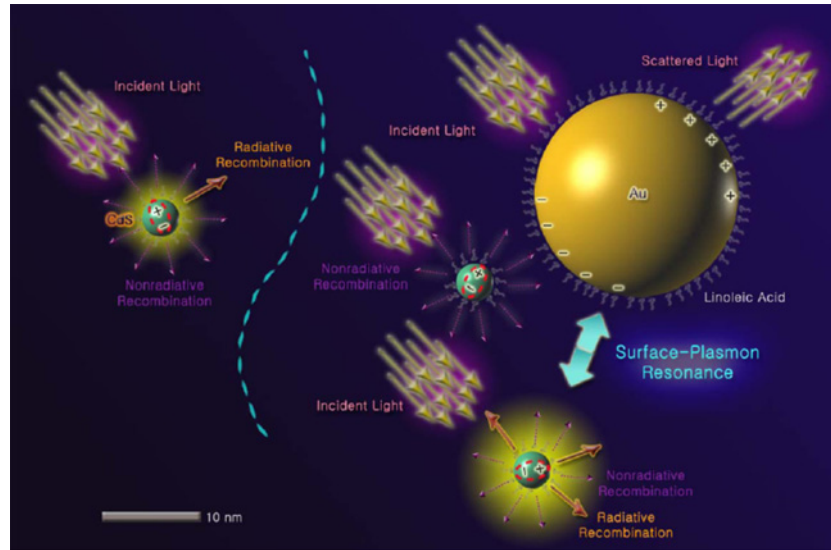


**Fig. 13.** Schematic figure of the proposed mechanism of photoluminescence enhancement by surface-plasmon resonance. Reprinted with permission from B. Park.<sup>[51]</sup> Copyright 2011, American Institute of Physics.

### 2.3 Enhanced Photoluminescence of Semiconductor Nanoparticles on Metal/Insulator Nanocomposite Film

The photoluminescence of CdS nanoparticles was also measured on Au/SiO<sub>2</sub> nanocomposite film deposited by sputtering.<sup>[54]</sup> Co-sputtering of metal and insulator leads to the formation of a nanocomposite film composed of metal nanoclusters and surrounding insulator matrix.<sup>[55-60]</sup> As shown in Fig. 14, the photoluminescence intensities were enhanced with the incorporation of Au/SiO<sub>2</sub> nanocomposite

films. Since there have been few reports considering back reflection from the metal layer, it was necessary to separate only the surface-plasmon effect in the photoluminescence enhancement, not from the reflecting light making prolonged optical-path lengths.

Absorption spectra in Fig. 15 show that the plasmon peaks of the Au/SiO<sub>2</sub> film shift from ~500 nm to ~560 nm with increasing Au fraction. The 75% Au film shows a surface-plasmon peak at the wavelength of ~540 nm which matches

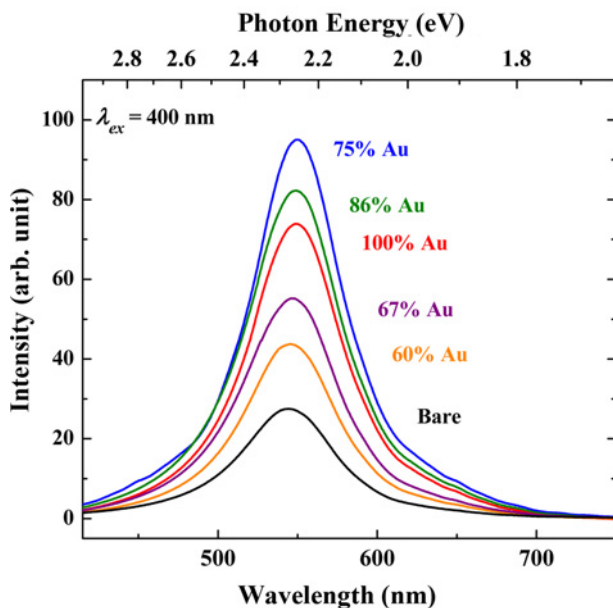


**Fig. 14.** Photoluminescence spectra of CdS nanoparticles with different Au fractions. Reprinted with permission from B. Park.<sup>[54]</sup> Copyright 2012, Elsevier.

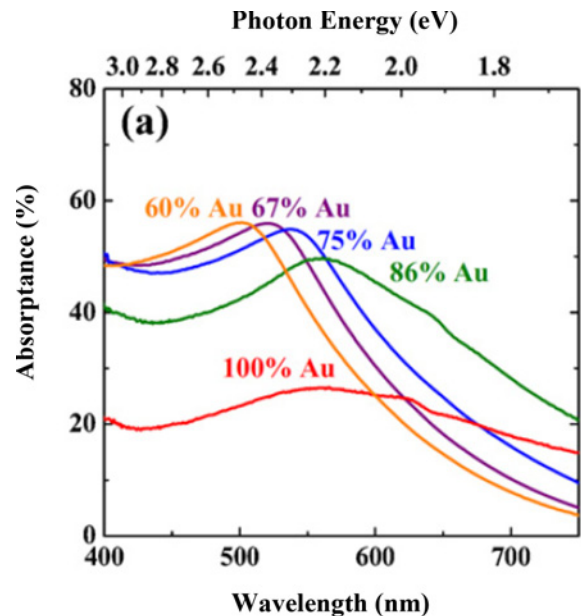


**Fig. 15.** Absorbance of Au/SiO<sub>2</sub> nanocomposites with various volume fractions of Au. Reprinted with permission from B. Park.<sup>[54]</sup> Copyright 2012, Elsevier.

well with the optimum photoluminescence (Fig. 14). The schematics of photoluminescence enhancement by the Au/SiO<sub>2</sub> surface-plasmon resonance is shown in Fig. 16.

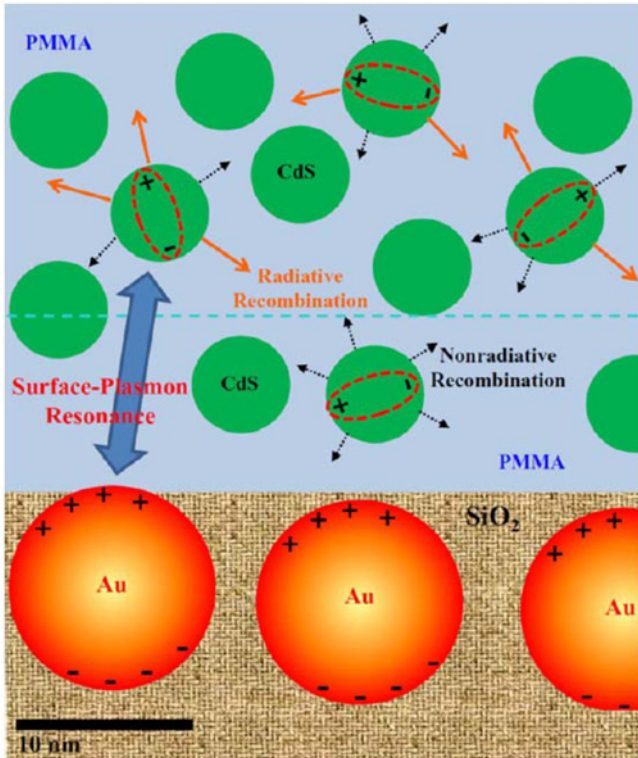


**Fig. 16.** Schematic figure of the proposed mechanism of photoluminescence enhancement by surface-plasmon resonance from Au/SiO<sub>2</sub> nanocomposites. Reprinted with permission from B. Park.<sup>[54]</sup> Copyright 2012, Elsevier.

**2.4 Density of Surface-Plasmon States and Luminescence Enhancement**

To study the effect of the density of surface-plasmon states on luminescence, CdS nanoparticles with various Au-film thicknesses were investigated.<sup>[61]</sup> As shown in Fig. 17(a), the photoluminescence efficiency was enhanced by increasing the Au layer thickness, and showed a tendency toward saturation after 100 nm. Furthermore, the luminescence efficiency was further increased by annealing the Au layer (Fig. 17(b)), probably due to the enhanced roughness produced by the thermal treatment.

The surface-plasmon relation can be obtained using Maxwell’s equations in a three-layer system (the inset of Fig. 17). The surface-plasmon dispersion relation at the Au/PMMA interface for various Au film thicknesses are derived from a dispersion equation, and can be shown as

$$\frac{\gamma_2 \epsilon_3}{\gamma_3 \epsilon_2} + \frac{(\epsilon_1 \gamma_2 + \epsilon_2 \gamma_1) + (\epsilon_1 \gamma_2 - \epsilon_2 \gamma_1) \exp(-2\gamma_2 t)}{(\epsilon_1 \gamma_2 + \epsilon_2 \gamma_1) + (\epsilon_1 \gamma_2 - \epsilon_2 \gamma_1) \exp(-2\gamma_2 t)} = 0 \quad (2-2)$$

where  $\epsilon_i$  and  $\gamma_i$  ( $\gamma_i^2 = k^2 - k_0^2 \epsilon_i$ ) are the dielectric constant and decay constant for material  $i$ , respectively ( $i = 1$  for glass, 2 for Au, and 3 for PMMA), and  $t$  is the thickness of the Au film. Figure 18 shows the derived dispersion relation of the metal/dielectric/semiconductor system. By differentiating  $E(k)$  with respect to  $k$ , the density of surface-plasmon states can be easily obtained as

$$\rho(\hbar\omega) = \frac{2\pi k L^2 dk}{(2\pi)^2 d(\hbar\omega) L^2} \frac{1}{L^2} = \frac{d(k^2)}{4\pi d(\hbar\omega)}. \quad (2-3)$$

The density of surface-plasmon states as a function of photon energy (inset of Fig. 18) increased with the increased Au film thickness, which can be correlated with the

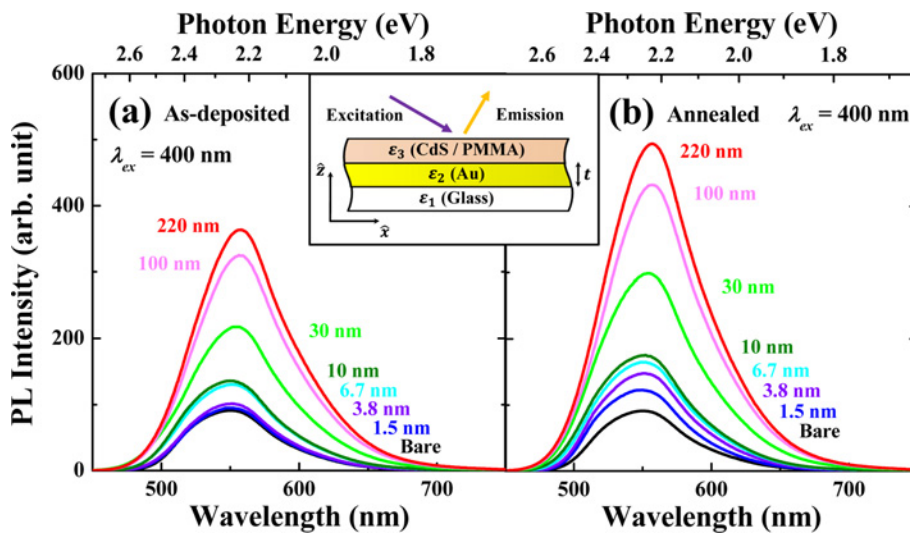


**Fig. 17.** Photoluminescence spectra of CdS nanoparticles with different thicknesses of Au film: (a) as-deposited and (b) annealed at 400°C for 30 min. The inset shows a schematic figure of a sample geometry and photoluminescence configuration. Reprinted with permission from B. Park.<sup>[61]</sup> Copyright 2012, Elsevier.

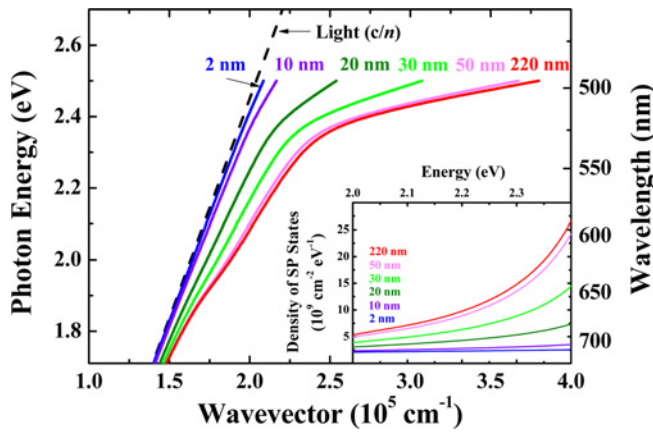


**Fig. 18.** Dispersion relation of surface plasmon at a planar Au/PMMA interface of a three-layer system for various Au film thicknesses. The light line in PMMA (index of refraction  $n \cong 1.61$ ) is shown as a dashed line. The inset shows the calculated density of surface-plasmon (SP) states as a function of photon energy for different Au thicknesses. Reprinted with permission from B. Park.<sup>[61]</sup> Copyright 2012, Elsevier.

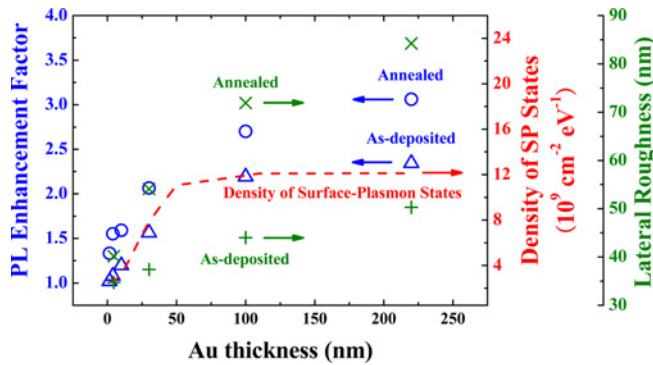


**Fig. 19.** The calculated PL enhancement factor and lateral roughness as a function of nominal thickness of Au film with and without annealing. The density of surface-plasmon (SP) states at 2.25 eV is shown as a dashed line. Reprinted with permission from B. Park.<sup>[61]</sup> Copyright 2012, Elsevier.

photoluminescence enhancement. Furthermore, by annealing the metal film to form a rough surface morphology, the CdS emission was further enhanced by the improved excitation and coupling of the surface-plasmon modes, as summarized in Fig. 19.

### 3. ENHANCED LIGHT ABSORPTION OF DYE MOLECULES BY LOCALIZED PLASMON RESONANCE IN SOLAR CELL

#### 3.1 Introduction

The localized-field enhancement by the nearby metal nanoparticles can be effectively utilized for light harvesting in various solar cells.<sup>[62-74]</sup> By a localized surface plasmon, the electromagnetic field near metal nanoparticles can be

amplified, and therefore more photons are absorbed with the same semiconductor-absorber thickness.<sup>[75]</sup> While there are many reports regarding nanostructured metals for the purpose of absorbing more light in solar cells by surface plasmon, the enhanced light absorption can also be achieved by light scattering from the submicron-sized metal particles.<sup>[76-80]</sup> Therefore, the separation of the field-enhancement effect from the light scattering (optical-path lengths) is necessary both for better understanding of the surface plasmon itself and for the practical application to solar-cell design. The nanoporous photoelectrode of a sensitized solar cell<sup>[81-98]</sup> is a suitable system to incorporate metal nanostructures and thereby to study plasmonic effects on the photovoltaic properties.

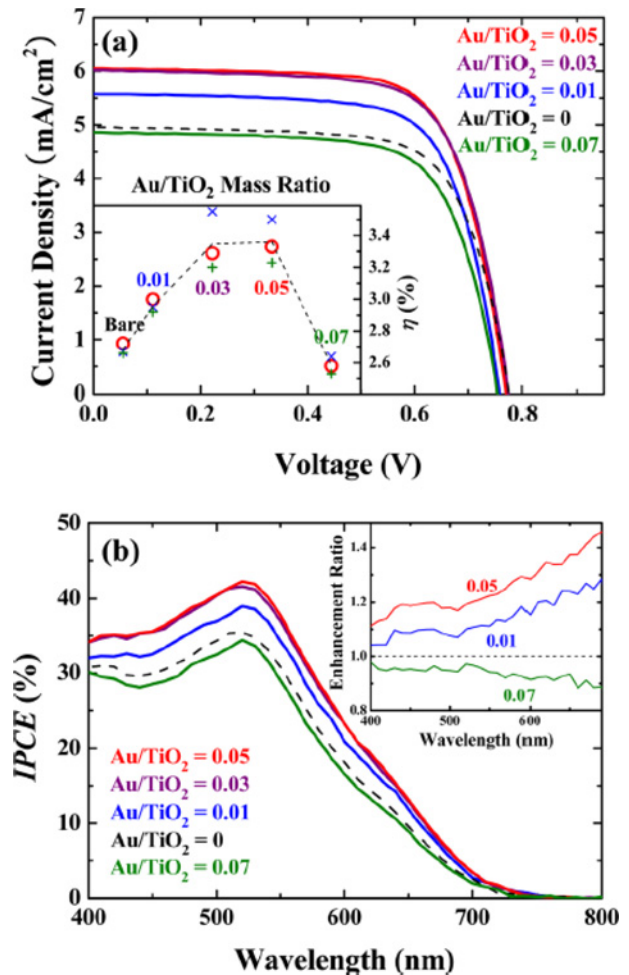


**Fig. 20.** (a) Photocurrent density-voltage characteristics of DSSCs at various Au/TiO<sub>2</sub> mass ratios. The inset shows the power-conversion efficiency of DSSCs with respect to the Au/TiO<sub>2</sub> mass ratio. (b) Incident photon-to-current conversion efficiency (IPCE) spectra of DSSCs at various Au/TiO<sub>2</sub> mass ratios. The IPCE-enhancement ratios are also shown compared with the bare DSSC (Au/TiO<sub>2</sub> = 0) in the inset. Reprinted with permission from B. Park.<sup>[99]</sup> Copyright 2011, American Institute of Physics.



### 3.2 The Effects of 100 nm-Diameter Au Nanoparticles in Sensitized Solar Cell

The effect of incorporating gold-nanoparticles in a dye-sensitized solar cell (DSSC) was investigated.<sup>[99]</sup> Approximately 100 nm-diameter Au nanoparticles were mixed with TiO<sub>2</sub>-nanoparticulate photoelectrode, and then dye molecules were chemisorbed onto the TiO<sub>2</sub> nanoparticle surface. Figure 20 shows the current density-voltage (*J-V*) curves and the incident photon-to-current conversion efficiency (*IPCE*) spectra of solar cells as a function of Au/TiO<sub>2</sub> mass ratios. The enhanced power-conversion efficiency ( $\eta$ ) of solar cells is attributed to the increased current density, which comes from the increased light absorption of the dye molecules, and is consistent with the *IPCE* data.

The extinction and diffused reflectance of the Au/TiO<sub>2</sub> film were measured to separate the scattering effect from the field-enhancement effect of the Au nanoparticles, since extinction represents a degree of both absorption and reflection. The definition of extinction is as follows:

$$\text{extinction} = -\log(I/I_0) = -\log T \tag{3-1}$$

$$A + R + T = 1 \tag{3-2}$$

where *A*, *R*, and *T* are absorptance, diffused reflectance, and transmittance, respectively.

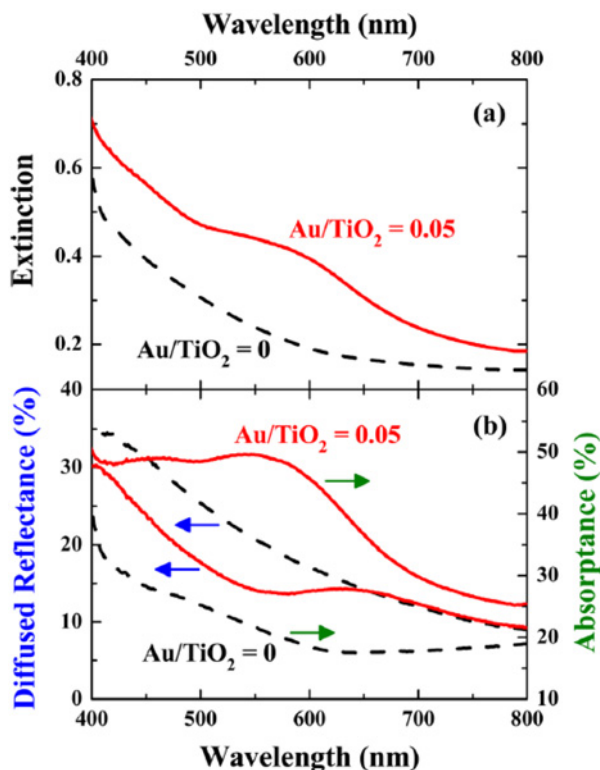


**Fig. 21.** (a) Extinction of Au/TiO<sub>2</sub> film (solid-red line) and TiO<sub>2</sub> film (dashed-black line) before dye adsorption. (b) Diffused reflectance (blue arrows) and absorptance (green arrows) of films before dye adsorption. Reprinted with permission from B. Park.<sup>[99]</sup> Copyright 2011, American Institute of Physics.

As shown in Fig. 21, the Au/TiO<sub>2</sub> film (without dye adsorption) exhibits higher extinction compared to the bare TiO<sub>2</sub> film with lower reflectance. This indicates that the higher total extinction at the wavelength of the surface-plas-

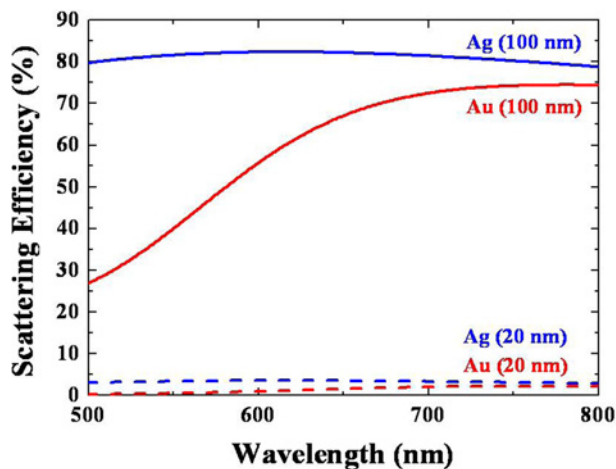


**Fig. 22.** Calculated scattering efficiency of Au and Ag nanoparticles. Dielectric function of medium ( $\epsilon_d$ ) was assumed as  $2 + 0 \cdot i$ . Reprinted with permission from B. Park.<sup>[99]</sup> Copyright 2011, American Institute of Physics.

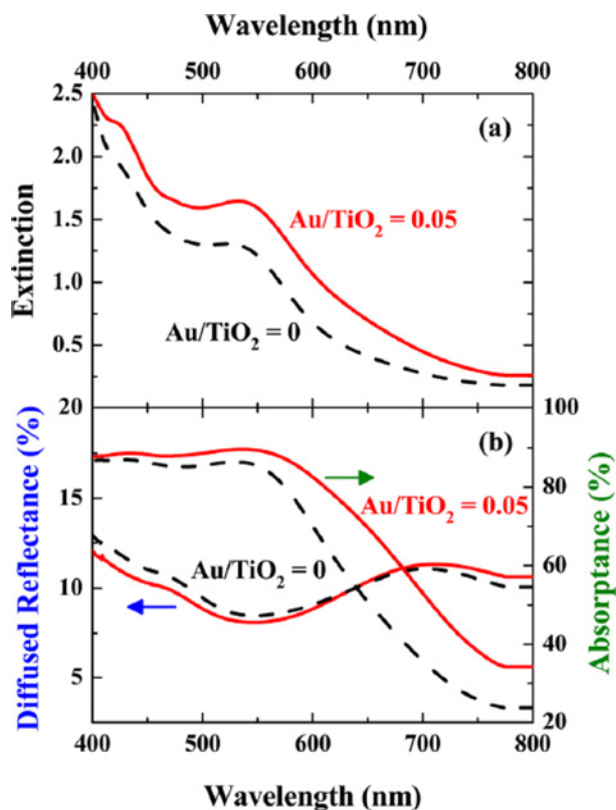


**Fig. 23.** (a) Extinction of Au/TiO<sub>2</sub> film (solid-red line) and TiO<sub>2</sub> film (dashed-black line) after dye adsorption. (b) Diffused reflectance (blue arrows) and absorptance (green arrows) of films after dye adsorption. Reprinted with permission from B. Park.<sup>[99]</sup> Copyright 2011, American Institute of Physics.

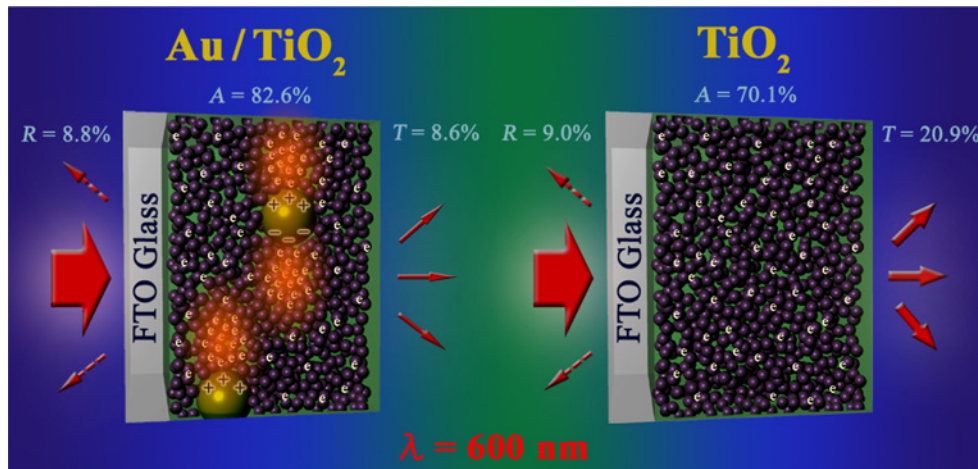


**Fig. 24.** Schematic figure representing the enhancement of Au/TiO<sub>2</sub>-DSSC. Field enhancement near the Au nanoparticles is depicted as orange-color regions. Reprinted with permission from B. Park.<sup>[99]</sup> Copyright 2011, American Institute of Physics.

mon resonance is attributed to the absorption, and confirms that the scattering effect is negligible. This is consistent with the calculated scattering efficiency of Ag and Au nanoparticles (Fig. 22). Unlike Ag, the Au nanoparticles exhibit a dominant absorption-nature as opposed to scattering at the wavelength of surface-plasmon resonance, which confirms the strong absorption by field enhancement in the case of Au/TiO<sub>2</sub> film.

Optical properties were also measured with the dye-attached Au/TiO<sub>2</sub> photoelectrode. As shown in Fig. 23, the dye-absorbed Au/TiO<sub>2</sub> film exhibits stronger extinction with similar reflectance spectra. The resultant absorbance data considering the extinction and the reflectance shows that the incorporation of Au nanoparticles into the TiO<sub>2</sub> electrode helps to absorb more light with the same dye amount by local-field enhancement.

The surface-plasmon resonance of an Au nanoparticle can also induce quenching processes by the energy transfer between dye and metal nanoparticle. However, the time constant for electron transfer from the dye to the TiO<sub>2</sub> electrode ( $\sim 1$  ps)<sup>[100-104]</sup> is much shorter than that for quenching by metal nanoparticle ( $\sim 100$  ps).<sup>[43-46]</sup> Therefore, the quenching effect is believed to be negligible in DSSC. Figure 24 shows a schematic illustration of the effect of a surface plasmon for enhanced power-conversion efficiency in a solar cell. When the metal nanoparticle is located close to the dye molecules in the solar cell structure, more light can be trapped by the dye absorber due to the localized-field enhancement from Au nanoparticles, and thereby more photoelectrons can be collected in the electrode.

#### 4. FUTURE WORK

Further studies are required to investigate the surface-plasmon effects on photoluminescence, such as the theoretical

approaches to the radiative recombination rates considering the electrodynamic interactions between semiconductor and metal nanoparticle, and the nonradiative recombination rates based on the energy-transfer rate between single exciton and surface-plasmon band as a function of metal-semiconductor distance. The additional complex plasmon influences by multiple metal nanoparticles should also be investigated. Moreover, the quantitative relation between the density of surface-plasmon states and metal nanostructures needs to be identified. For the more practical applications of surface plasmons in luminescence and solar-cell structures, a theory for the effect of absorber-metal distance and the size/shape/concentration effects of metal nanostructures needs to be understood, for optimum efficiency in both applications.

#### ACKNOWLEDGMENTS

This research was supported by the National Research Foundation of Korea, through the World Class University (WCU, R31-2008-000-10075-0) and the Korean Government (MEST: NRF, 2010-0029065), and by the Center for Iron and Steel Research (0417-20120001).

#### REFERENCES

1. W. L. Barnes, A. Dereux, and T. W. Ebbesen, "Surface Plasmon Subwavelength Optics," *Nature* **424**, 824 (2003).
2. W. L. Barnes, "Turning the Tables on Surface Plasmons," *Nat. Mater.* **3**, 588 (2004).
3. C. F. Bohren and D. R. Huffman, *Absorption and Scattering of Light by Small Particles*, p. 340, Wiley, New York (1983).
4. S. C. Erwin, L. Zu, M. I. Haftel, A. L. Efros, T. A. Kennedy, and D. J. Norris, "Doping Semiconductor Nanocrystals," *Nature* **436**, 91 (2005).

5. V. L. Colvin, M. C. Schlamp, and A. P. Alivisatos, "Light-Emitting Diodes Made from Cadmium Selenide Nanocrystals and a Semiconducting Polymer," *Nature* **370**, 354 (1994).
6. R. N. Bhargava and D. Gallagher, "Optical Properties of Manganese-Doped Nanocrystals of ZnS," *Phys. Rev. Lett.* **72**, 416 (1994).
7. D.-R. Jung, J. Kim, and B. Park, "Surface-Passivation Effects on the Photoluminescence Enhancement in ZnS:Mn Nanoparticles by Ultraviolet Irradiation with Oxygen Bubbling," *Appl. Phys. Lett.* **96**, 211908 (2010).
8. D.-R. Jung, D. Son, J. Kim, C. Kim, and B. Park, "Highly Luminescent Surface-Passivated ZnS:Mn nanoparticles by a Simple One-Step Synthesis," *Appl. Phys. Lett.* **93**, 163188 (2008).
9. D. Son, D.-R. Jung, J. Kim, T. Moon, C. Kim, and B. Park, "Synthesis and Photoluminescence of Mn-Doped Zinc Sulfide Nanoparticles," *Appl. Phys. Lett.* **90**, 101910 (2007).
10. N. S. Norberg and D. R. Gamelin, "Influence of Surface Modification on the Luminescence of Colloidal ZnO Nanocrystals," *J. Phys. Chem. B* **109**, 20810 (2005).
11. P. V. Radovanovic, N. S. Norberg, K. E. McNally, and D. R. Gamelin, "Colloidal Transition-Metal-Doped ZnO Quantum Dots," *J. Am. Chem. Soc.* **124**, 15192 (2002).
12. M. L. Pang, W. Y. Shen, and J. Lin, "Enhanced Photoluminescence of  $\text{Ga}_2\text{O}_3:\text{Dy}^{3+}$  Phosphor Films by  $\text{Li}^+$  Doping," *J. Appl. Phys.* **97**, 033511 (2005).
13. J. Y. Cho, Y. R. Do, and Y.-D. Huh, "Analysis of the Factors Governing the Enhanced Photoluminescence Brightness of Li-Doped  $\text{Y}_2\text{O}_3:\text{Eu}$  Thin-Film Phosphors," *Appl. Phys. Lett.* **89**, 131915 (2006).
14. A. A. Bol and A. Meijerink, "Luminescence Quantum Efficiency of Nanocrystalline  $\text{ZnS}:\text{Mn}^{2+}$ : 2. Enhancement by UV Irradiation," *J. Phys. Chem. B* **105**, 10203 (2001).
15. H. Yang and P. H. Holloway, "Efficient and Photostable ZnS-Passivated CdS:Mn Luminescent Nanocrystals," *Adv. Funct. Mater.* **14**, 152 (2004).
16. V. Biju, R. Kanemoto, Y. Matsumoto, S. Ishii, S. Nakanishi, T. Itoh, Y. Baba, and M. Ishikawa, "Photoinduced Photoluminescence Variations of CdSe Quantum Dots in Polymer Solutions," *J. Phys. Chem. C* **111**, 7924 (2007).
17. X. Wang, L. Qu, J. Zhang, X. Peng, and M. Xiao, "Surface-Related Emission in Highly Luminescent CdSe Quantum Dots," *Nano Lett.* **3**, 1103 (2003).
18. C. Carrillo-Carrión, S. Cárdenas, B. M. Simonet, and M. Valcárcel, "Quantum Dots Luminescence Enhancement due to Illumination with UV/Vis Light," *Chem. Commun.* 5214 (2009).
19. K. T. Shimizu, W. K. Woo, B. R. Fisher, H. J. Eisler, and M. G. Bawendi, "Surface-Enhanced Emission from Single Semiconductor Nanocrystals," *Phys. Rev. Lett.* **89**, 117401 (2002).
20. M. Mattila, T. Hakkarainen, H. Lipsanen, H. Jiang, and E. I. Kauppinen, "Enhanced Luminescence from Catalyst-Free Grown InP Nanowires," *Appl. Phys. Lett.* **90**, 033101 (2007).
21. N. Myung, Y. Bae, and A. J. Bard, "Enhancement of the Photoluminescence of CdSe Nanocrystals Dispersed in  $\text{CHCl}_3$  by Oxygen Passivation of Surface States," *Nano Lett.* **3**, 747 (2003).
22. J. Zhuang, X. Zhang, G. Wang, D. Li, W. Yang, and T. Li, "Synthesis of Water-Soluble  $\text{ZnS}:\text{Mn}^{2+}$  Nanocrystals by Using Mercaptopropionic Acid as Stabilizer," *J. Mater. Chem.* **13**, 1853 (2003).
23. E. Jang, S. Jun, Y. Chung, and L. Pu, "Surface Treatment to Enhance the Quantum Efficiency of Semiconductor Nanocrystals," *J. Phys. Chem. B* **108**, 4597 (2004).
24. H. Yang, P. H. Holloway, G. Cunningham, and K. S. Schanze, "CdS:Mn Nanocrystals Passivated by ZnS: Synthesis and Luminescent Properties," *J. Chem. Phys.* **121**, 10233 (2004).
25. M.-K. Kwon, J.-Y. Kim, B.-H. Kim, I.-K. Park, C.-Y. Cho, C. C. Byeon, and S.-J. Park, "Surface-Plasmon-Enhanced Light-Emitting Diodes," *Adv. Mater.* **20**, 1253 (2008).
26. O. G. Tovmachenko, C. Graf, D. J. van den Hauvel, A. van Blaaderen, and H. C. Gerritsen, "Fluorescence Enhancement by Metal-Core/Silica-Shell nanoparticles," *Adv. Mater.* **18**, 91 (2006).
27. M.-S. Hu, H.-L. Chen, C.-H. Shen, L.-S. Hong, B.-R. Huang, K.-H. Chen, and L.-C. Chen, "Photosensitive Gold-nanoparticle-Embedded Dielectric Nanowires," *Nat. Mater.* **5**, 102 (2006).
28. H. S. Jang, H. Yang, S. W. Kim, J. Y. Han, S.-G. Lee, and D. Y. Jeon, "White Light-Emitting Diodes with Excellent Color Rendering Based on Organically Capped CdSe Quantum Dots and  $\text{Sr}_3\text{SiO}_5:\text{Ce}^{3+},\text{Li}^+$  Phosphors," *Adv. Mater.* **20**, 2696 (2008).
29. T.-G. Kim, Y.-W. Kim, J. S. Kim, and B. Park, "Silver-Nanoparticle Dispersion from the Consolidation of Ag-Attached Silica Colloid," *J. Mater. Res.* **19**, 1400 (2004).
30. K. H. Cho, S. I. Ahn, S. M. Lee, C. S. Choi, and K. C. Choi, "Surface Plasmonic Controllable Enhanced Emission from the Intrachain and Interchain Excitons of a Conjugated Polymer," *Appl. Phys. Lett.* **97**, 193306 (2010).
31. P. P. Pompa, L. Martiradonna, A. D. Torre, F. D. Sala, L. Manna, M. D. Vittorio, F. Calabi, B. Cingolani, and R. Rinaldi, "Metal-Enhanced Fluorescence of Colloidal Nanocrystals with Nanoscale Control," *Nat. Nanotechnol.* **1**, 126 (2006).
32. Y. Ito, K. Matsuda, and Y. Kanemitsu, "Mechanism of Photoluminescence Enhancement in Single Semiconductor Nanocrystals on Metal Surfaces," *Phys. Rev. B* **75**, 033309 (2007).
33. L. M. Liz-Marzan, "Tailoring Surface Plasmons through the Morphology and Assembly of Metal Nanoparticles," *Langmuir* **22**, 32 (2006).
34. M.-K. Lee, T. G. Kim, W. Kim, and Y.-M. Sung, "Surface

- Plasmon Resonance (SPR) Electron and Energy Transfer in Noble Metal-Zinc Oxide Composite Nanocrystals,” *J. Phys. Chem. C* **112**, 10079 (2008).
35. J. S. Biteen, L. A. Sweatlock, H. Mertens, N. S. Lewis, A. Polman, and H. A. Atwater, “Plasmon-Enhanced Photoluminescence of Silicon Quantum Dots: Simulation and Experiment,” *J. Phys. Chem. C* **111**, 13372 (2007).
  36. Y.-C. Lu, C.-Y. Chen, C. K.-C. Shen, D.-M. Yeh, T.-Y. Tang, and C. C. Yang, “Enhanced Photoluminescence Excitation in Surface Plasmon Coupling with an InGaN/GaN Quantum Well,” *Appl. Phys. Lett.* **91**, 183107 (2004).
  37. K. Okamoto, I. Niki, A. Scherer, Y. Narukawa, T. Mukai, and Y. Kawakami, “Surface Plasmon Enhanced Spontaneous Emission Rate of InGaN/GaN Quantum Wells Probed by Time-Resolved Photoluminescence Spectroscopy,” *Appl. Phys. Lett.* **87**, 071102 (2005).
  38. K. Okamoto, I. Niki, A. Shvartser, Y. Narukawa, T. Mukai, and A. Scherer, “Surface-Plasmon-Enhanced Light Emitters Based on InGaN Quantum Wells,” *Nat. Mater.* **3**, 601 (2004).
  39. K. Tanabe, “Field Enhancement around Metal Nanoparticles and Nanoshells: a Systematic Investigation,” *J. Phys. Chem. C* **112**, 15721 (2008).
  40. D.-R. Jung, J. Kim, C. Nahm, H. Choi, S. Nam, and B. Park, “Review paper: Semiconductor Nanoparticles with Surface Passivation and Surface Plasmon,” *Electron. Mater. Lett.* **7**, 185 (2011).
  41. S. D. Standridge, G. C. Schatz, and J. T. Hupp, “Distance Dependence of Plasmon-Enhanced Photocurrent in Dye-Sensitized Solar Cells,” *J. Am. Chem. Soc.* **131**, 8407 (2009).
  42. A. O. Govorov and I. Carmeli, “Hybrid Structures Composed of Photosynthetic System and Metal Nanoparticles: Plasmon Enhancement Effect,” *Nano Lett.* **7**, 620 (2007).
  43. A. O. Govorov, G. W. Bryant, W. Zhang, T. Skeini, J. Lee, N. A. Kotov, J. M. Slocik, and R. R. Naik, “Exciton-Plasmon Interaction and Hybrid Excitons in Semiconductor-Metal Nanoparticle Assemblies,” *Nano Lett.* **6**, 984 (2006).
  44. E. Dulkeith, M. Ringle, T. A. Klar, J. Feldmann, A. Munoz Javier, and W. J. Parak, “Gold Nanoparticles Quench Fluorescence by Phase Induced Radiative Rate Suppression,” *Nano Lett.* **5**, 585 (2005).
  45. Z. Gueroui and A. Libchaber, “Single-Molecule Measurements of Gold-Quenched Quantum Dots,” *Phys. Rev. Lett.* **93**, 166108 (2004).
  46. J. M. Slocik, A. O. Govorov, and R. R. Naik, “Optical Characterization of Bio-Assembled Hybrid Nanostructures,” *Supramol. Chem.* **18**, 415 (2006).
  47. S. Pan and L. J. Rothberg, “Enhancement of Platinum Octaethyl Prophyrin Phosphorescence near Nanotextured Silver Surfaces,” *J. Am. Chem. Soc.* **127**, 6087 (2005).
  48. S. Mackowski, S. Wörmke, A. J. Maier, T. H. P. Brotsudarmo, H. Harutyunyan, A. Hartschuh, A. O. Govorov, H. Scheer, and C. Bräuchle, “Metal-Enhanced Fluorescence of Chlorophylls in Single Light-Harvesting Complexes,” *Nano Lett.* **8**, 558 (2008).
  49. J. Lee, A. O. Govorov, J. Dulka, and N. A. Kotov, “Bioconjugates of CdTe Nanowires and Au Nanoparticles: Plasmon-Exciton Interactions, Luminescence Enhancement, and Collective Effects,” *Nano Lett.* **4**, 2323 (2004).
  50. P. Anger, P. Bharadwaj, and L. Novotny, “Enhancement and Quenching of Single-Molecule Fluorescence,” *Phys. Rev. Lett.* **96**, 113002 (2006).
  51. D.-R. Jung, J. Kim, S. Nam, C. Nahm, H. Choi, J. I. Kim, J. Lee, C. Kim, and B. Park, “Photoluminescence Enhancement in CdS Nanoparticles by Surface-Plasmon Resonance,” *Appl. Phys. Lett.* **99**, 041906 (2011).
  52. K. Aslan, M. Wu, J. R. Lakowicz, and C. D. Geddes, “Fluorescent Core-Shell Ag@SiO<sub>2</sub> Nanocomposites for Metal-Enhanced Fluorescence and Single Nanoparticle Sensing Platforms,” *J. Am. Chem. Soc.* **129**, 1524 (2007).
  53. O. Kulakovich, N. Strekal, A. Yaroshevich, S. Maskevich, S. Gaponenko, I. Nabiev, U. Woggon, and M. Artemyev, “Enhanced Luminescence of CdSe Quantum Dots on Gold Colloids,” *Nano Lett.* **2**, 1449 (2002).
  54. D.-R. Jung, J. Kim, C. Nahm, S. Nam, J. I. Kim, and B. Park, “Surface-Plasmon-Enhanced Photoluminescence of CdS Nanoparticles with Au/SiO<sub>2</sub> Nanocomposites,” *Mater. Res. Bull.* **47**, 453 (2012).
  55. Y. Park, B. Lee, C. Kim, J. Kim, S. Nam, Y. Oh, and B. Park, “Modification of Gold Catalysis with Aluminum Phosphate for Oxygen-Reduction Reaction,” *J. Phys. Chem. C* **114**, 3688 (2010).
  56. B. Lee, C. Kim, Y. Park, T.-G. Kim, and B. Park, “Nanostructured Platinum/Iron-Phosphate Thin-Film Electrodes for Methanol Oxidation,” *Electrochem. Solid-State Lett.* **9**, E27 (2006).
  57. Y. Oh, J. Kang, S. Nam, S. Byun, and B. Park, “Pt/AlPO<sub>4</sub> Nanocomposite Thin-Film Electrodes for Ethanol Electrooxidation,” *Mater. Chem. Phys.* **135**, 188 (2012).
  58. J. Park, Y. Oh, Y. Park, S. Nam, J. Moon, J. Kang, D.-R. Jung, S. Byun, and B. Park, “Methanol Oxidation in Nanostructured Platinum/Cerium-Phosphate Thin Films,” *Curr. Appl. Phys.* **11**, S2 (2011).
  59. S. J. Yoo, T.-Y. Jeon, Y.-H. Cho, K.-S. Lee, and Y.-E. Sung, “Particle Size Effects of PtRu Nanoparticles Embedded in TiO<sub>2</sub> on Methanol Electrooxidation,” *Electrochim. Acta* **55**, 7939 (2010).
  60. J. W. Lim, S. J. Yoo, S. H. Park, S. U. Yun, and Y.-E. Sung, “High Electrochromic Performance of co-Sputtered Vanadium-Titanium Oxide as a Counter Electrode,” *Sol. Energy Mater. Sol. Cells* **93**, 2069 (2009).
  61. J. I. Kim, D.-R. Jung, J. Kim, C. Nahm, S. Byun, S. Lee, and B. Park, “Surface-Plasmon-Coupled Photoluminescence from CdS Nanoparticles with Au Films,” *Solid State Commun.* (2012). [DOI:10.1016/j.ssc.2012.05.008]
  62. J.-L. Wu, F.-C. Chen, Y.-S. Hsiao, F.-C. Chien, P. Chen,

- C.-H. Kuo, M. H. Huang, and C.-S. Hsu, "Surface Plasmonic Effects of Metallic Nanoparticles on the Performance of Polymer Bulk Heterojunction Solar Cells," *ACS Nano* **5**, 959 (2011).
63. B. P. Rand, P. Peumans, and S. R. Forrest, "Long-Range Absorption Enhancement in Organic Tandem Thin-Film Solar Cells Containing Silver Nanoclusters," *J. Appl. Phys.* **96**, 7519 (2004).
64. A. J. Morfa, K. L. Rowlen, T. H. Reily, M. J. Romero, and J. van de Lagemaat, "Plasmon-Enhanced Solar Energy Conversion in Organic Bulk Heterojunction Photovoltaics," *Appl. Phys. Lett.* **92**, 013504 (2008).
65. J. K. Mapel, M. Singh, M. A. Baldo, and K. Celebi, "Plasmonic Excitation of Organic Double Heterostructure Solar Cells," *Appl. Phys. Lett.* **90**, 121102 (2007).
66. S.-S. Kim, S.-I. Na, J. Jo, D.-Y. Kim, and Y.-C. Nah, "Plasmon Enhanced Performance of Organic Solar Cells Using Electrodeposited Ag nanoparticles," *Appl. Phys. Lett.* **93**, 073307 (2008).
67. J. Qi, X. Dang, P. T. Hammond, and A. M. Belcher, "Highly Efficient Plasmon-Enhanced Dye-Sensitized Solar Cells through Metal@Oxide Core-Shell Nanostructure," *ACS Nano* **5**, 7108 (2011).
68. J. Du, J. Qi, D. Wang, and Z. Tang, "Facile Synthesis of Au@TiO<sub>2</sub> Core-Shell Hollow Spheres for Dye-Sensitized Solar Cells with Remarkably Improved Efficiency," *Energy Environ. Sci.* **5**, 6914 (2012).
69. M. Westphalen, U. Kreibitz, J. Rostalski, H. Lüth, and D. Meissner, "Metal Cluster Enhanced Organic Solar Cells," *Sol. Energy Mater. Sol. Cells* **61**, 97 (2000).
70. S. D. Standridge, G. C. Schatz, and J. T. Hupp, "Toward Plasmonic Solar Cells: Protection of Silver Nanoparticles via Atomic Layer Deposition of TiO<sub>2</sub>," *Langmuir* **25**, 2596 (2009).
71. M. D. Brown, T. Suteewong, R. S. S. Kumar, V. D'Innocenzo, A. Petrozza, M. Lee, U. Wiesner, and H. J. Snaith, "Plasmonic Dye-Sensitized Solar Cells Using Core-Shell Metal-Insulator Nanoparticles," *Nano Lett.* **11**, 438 (2011).
72. B. Ding, B. J. Lee, M. Yang, H. S. Jung, and J.-K. Lee, "Surface-Plasmon Assisted Energy Conversion in Dye-Sensitized Solar Cells," *Adv. Energy Mater.* **1**, 415 (2011).
73. C. Hägglund, M. Zäch, and B. Kasemo, "Enhanced Charge Carrier Generation in Dye Sensitized Solar Cells by Nanoparticle Plasmons," *Appl. Phys. Lett.* **92**, 013113 (2008).
74. M. Ihara, M. Kanno, and S. Inoue, "Photoabsorption-Enhanced Dye-Sensitized Solar Cell by Using Localized Surface Plasmon of Silver Nanoparticles Modified with Polymer," *Physica E* **42**, 2867 (2010).
75. H. A. Atwater and A. Polman, "Plasmonics for Improved Photovoltaic Devices," *Nat. Mater.* **9**, 205 (2010).
76. D. M. Schaadt, B. Feng, and E. T. Yu, "Enhanced Semiconductor Optical Absorption via Surface Plasmon Excitation in Metal Nanoparticles," *Appl. Phys. Lett.* **86**, 063106 (2005).
77. D. Derkacs, S. H. Lim, P. Matheu, W. Mar, and E. T. Yu, "Improved Performance of Amorphous Silicon Solar Cells via Scattering from Surface Plasmon Polaritons in nearby Metallic Nanoparticles," *Appl. Phys. Lett.* **89**, 093103 (2006).
78. K. Nakayama, K. Tanabe, and H. A. Atwater, "Plasmonic Nanoparticle Enhanced Light Absorption in GaAs Solar Cells," *Appl. Phys. Lett.* **93**, 121904 (2008).
79. S. Pillai, K. R. Catchpole, T. Trupke, and M. A. Green, "Surface Plasmon Enhanced Silicon Solar Cells," *J. Appl. Phys.* **101**, 093105 (2007).
80. I.-K. Ding, J. Zhu, W. Cai, S.-J. Moon, N. Cai, P. Wang, S. M. Zakeeruddin, M. Grätzel, M. L. Brongersma, Y. Cui, and M. D. McGehee, "Plasmonic Dye-Sensitized Solar Cells," *Adv. Energy Mater.* **1**, 52 (2011).
81. B. O'Regan and M. Grätzel, "A Low-Cost, High-Efficiency Solar Cell Based on Dye-Sensitized Colloidal TiO<sub>2</sub> Films," *Nature* **353**, 737 (1991).
82. M. Grätzel, "Solar Energy Conversion by Dye-Sensitized Photovoltaic Cells," *Inorg. Chem.* **44**, 6841 (2005).
83. C. J. Barbé, F. Arendse, P. Comte, M. Jirousek, F. Lenzmann, V. Shklover, and M. Grätzel, "Nanocrystalline Titanium Oxide Electrodes for Photovoltaic Applications," *J. Am. Ceram. Soc.* **80**, 3157 (1997).
84. M. K. Nazeeruddin, A. Kay, I. Rodicio, R. Humphry-Baker, E. Müller, P. Liska, N. Vlachopoulos, and M. Grätzel, "Conversion of Light to Electricity by *cis*-X<sub>2</sub>Bis(2,2'-bipyridyl-4,4'-dicarboxylate)ruthenium(II) Charge-Transfer Sensitizers (X=Cl<sup>-</sup>, Br<sup>-</sup>, I<sup>-</sup>, CN<sup>-</sup>, and SCN<sup>-</sup>) on Nanocrystalline TiO<sub>2</sub> Electrodes," *J. Am. Chem. Soc.* **115**, 6382 (1993).
85. S. Ito, P. Chen, P. Comte, M. K. Nazeeruddin, P. Liska, P. Péchy, and M. Grätzel, "Fabrication of Screen-Printing Pastes from TiO<sub>2</sub> Powders for Dye-Sensitized Solar Cells," *Prog. Photovoltaics* **15**, 603 (2007).
86. M. K. Nazeeruddin, R. Humphry-Baker, and M. Grätzel, "Investigation of Sensitizer Adsorption and the Influence of Protons on Current and Voltage of a Dye-Sensitized Nanocrystalline TiO<sub>2</sub> Solar Cell," *J. Phys. Chem. B* **107**, 8981 (2003).
87. G. P. Smestad and M. Grätzel, "Demonstrating Electron Transfer and Nanotechnology: a Natural Dye-Sensitized Nanocrystalline Energy Converter," *J. Chem. Educ.* **75**, 752 (1998).
88. N.-G. Park, K. M. Kim, M. G. Kang, K. S. Ryu, S. H. Chang, and Y.-J. Shin, "Chemical Sintering of Nanoparticles: a Methodology for Low-Temperature Fabrication of Dye-Sensitized TiO<sub>2</sub> Films," *Adv. Mater.* **17**, 2349 (2005).
89. N.-G. Park, J. van de Lagemaat, and A. J. Frank, "Comparison of Dye-Sensitized Rutile- and Anatase-Based TiO<sub>2</sub> Solar Cells," *J. Phys. Chem. B* **104**, 8989 (2000).
90. N.-G. Park, G. Schlichthörl, J. van de Lagemaat, H. M.

- Cheong, A. Mascarenhas, and A. J. Frank, "Dye-Sensitized TiO<sub>2</sub> Solar Cells: Structural and Photoelectrochemical Characterization of Nanocrystalline Electrodes Formed from the Hydrolysis of TiCl<sub>4</sub>," *J. Phys. Chem. B* **103**, 3308 (1999).
91. N.-G. Park, M. G. Kang, K. M. Kim, K. S. Ryu, and S. H. Chang, "Morphological and Photoelectrochemical Characterization of Core-Shell Nanoparticle Films for Dye-Sensitized Solar Cells: Zn-O Type Shell on SnO<sub>2</sub> and TiO<sub>2</sub> Cores," *Langmuir* **20**, 4246 (2004).
92. P. M. Sommeling, B. C. O'Regan, R. R. Haswell, H. J. P. Smit, N. J. Bakker, J. J. T. Smits, J. M. Kroon, and J. A. M. van Roosmalen, "Influence of a TiCl<sub>4</sub> Post-Treatment on Nanocrystalline TiO<sub>2</sub> Films in Dye-Sensitized Solar Cells," *J. Phys. Chem. B* **110**, 19191 (2006).
93. S. Ito, P. Liska, P. Comte, R. Charvet, P. Péchy, U. Bach, L. Schmidt-Mende, S. M. Zakeeruddin, A. Kay, M. K. Nazeeruddin, and M. Grätzel, "Control of Dark Current in Photoelectrochemical (TiO<sub>2</sub>/I<sup>-</sup>/I<sub>3</sub><sup>-</sup>) and Dye-Sensitized Solar Cells," *Chem. Commun.* 4351 (2005).
94. S. Ito, T. N. Murakami, P. Comte, P. Liska, C. Grätzel, M. K. Nazeeruddin, and M. Grätzel, "Fabrication of Thin Film Dye Sensitized Solar Cells with Solar to Electric Power Conversion Efficiency over 10%," *Thin Solid Films* **516**, 4613 (2008).
95. H. Choi, C. Nahm, J. Kim, J. Moon, S. Nam, C. Kim, D.-R. Jung, and B. Park, "The Effect of TiCl<sub>4</sub>-Treated TiO<sub>2</sub> Compact Layer on the Performance of Dye-Sensitized Solar Cell," *Curr. Appl. Phys.* **12**, 737 (2012).
96. S. Rühle, M. Shalom, and A. Zaban, "Quantum-Dot-Sensitized Solar Cells," *ChemPhysChem* **11**, 2290 (2010).
97. G. Hodes, "Comparison of Dye- and Semiconductor-Sensitized Porous Nanocrystalline Liquid Junction Solar Cells," *J. Phys. Chem. C* **112**, 17778 (2008).
98. J. Kim, H. Choi, C. Nahm, J. Moon, C. Kim, S. Nam, D.-R. Jung, and B. Park, "The Effect of a Blocking Layer on the Photovoltaic Performance in CdS Quantum-Dot-Sensitized Solar Cells," *J. Power Sources* **196**, 10526 (2011).
99. C. Nahm, H. Choi, J. Kim, D.-R. Jung, C. Kim, J. Moon, B. Lee, and B. Park, "The Effects of 100 nm-Diameter Au nanoparticles on Dye-Sensitized Solar Cells," *Appl. Phys. Lett.* **99**, 253107 (2011).
100. A. Hagfeldt, G. Boschloo, L. Sun, L. Kloo, and H. Pettersson, "Dye-Sensitized Solar Cells," *Chem. Rev.* **110**, 6595 (2010).
101. D. Kuang, S. Ito, B. Wenger, C. Klein, J.-E. Moser, R. Humphry-Baker, S. M. Zakeeruddin, and M. Grätzel, "High Molar Extinction Coefficient Heteroleptic Ruthenium Complexes for Thin Film Dye-Sensitized Solar Cells," *J. Am. Chem. Soc.* **128**, 4146 (2006).
102. J. J. H. Pijpers, R. Ulbricht, S. Derossi, J. N. H. Reek, and M. Bonn, "Picosecond Electron Injection Dynamics in Dye-Sensitized Oxides in the Presence of Electrolyte," *J. Phys. Chem. C* **115**, 2578 (2011).
103. G. Benkö, J. Kallioinen, J. E. I. Korppi-Tommola, A. P. Yartsev, and V. Sundström, "Photoinduced Ultrafast Dye-to-Semiconductor Electron Injection from Nonthermalized and Thermalized Donor States," *J. Am. Chem. Soc.* **124**, 489 (2002).
104. J. Kim, H. Choi, C. Nahm, C. Kim, S. Nam, S. Kang, D.-R. Jung, J. I. Kim, J. Kang, and B. Park, "The Role of a TiCl<sub>4</sub> Treatment on the Performance of CdS Quantum-Dot-Sensitized Solar Cells," *J. Power Sources* **220**, 108 (2012).